Update on VDE Modeling with NIMROD

C. R. Sovinec and K. J. Bunkers

University of Wisconsin-Madison

Pre-APS CEMM Meeting

October 26, 2014

New Orleans, Louisiana

Summary

- Most of our progress since the TSD workshop in July has been in meshing external regions.
- We have also started running VDE computations with a realistic H-mode profile (conducting wall case, so far).
- Development for interfacing computational regions is also described.

Numerical modeling: A configuration is divided into separate computational regions.

- The inner region is an Eulerian representation of the plasma and internal vacuum.
- An arbitrary number of outer regions represent vacuum (curl-free) magnetic field only.
- Regions are separated by resistive surfaces using the thin-wall approximation.

$$\frac{\partial \mathbf{B}\cdot\hat{\mathbf{n}}}{\partial t} = -\hat{\mathbf{n}}\cdot\nabla\times\left[\left(\frac{\eta_w}{\mu_0 \delta x}\right)\hat{\mathbf{n}}\times\delta\mathbf{B}\right]$$

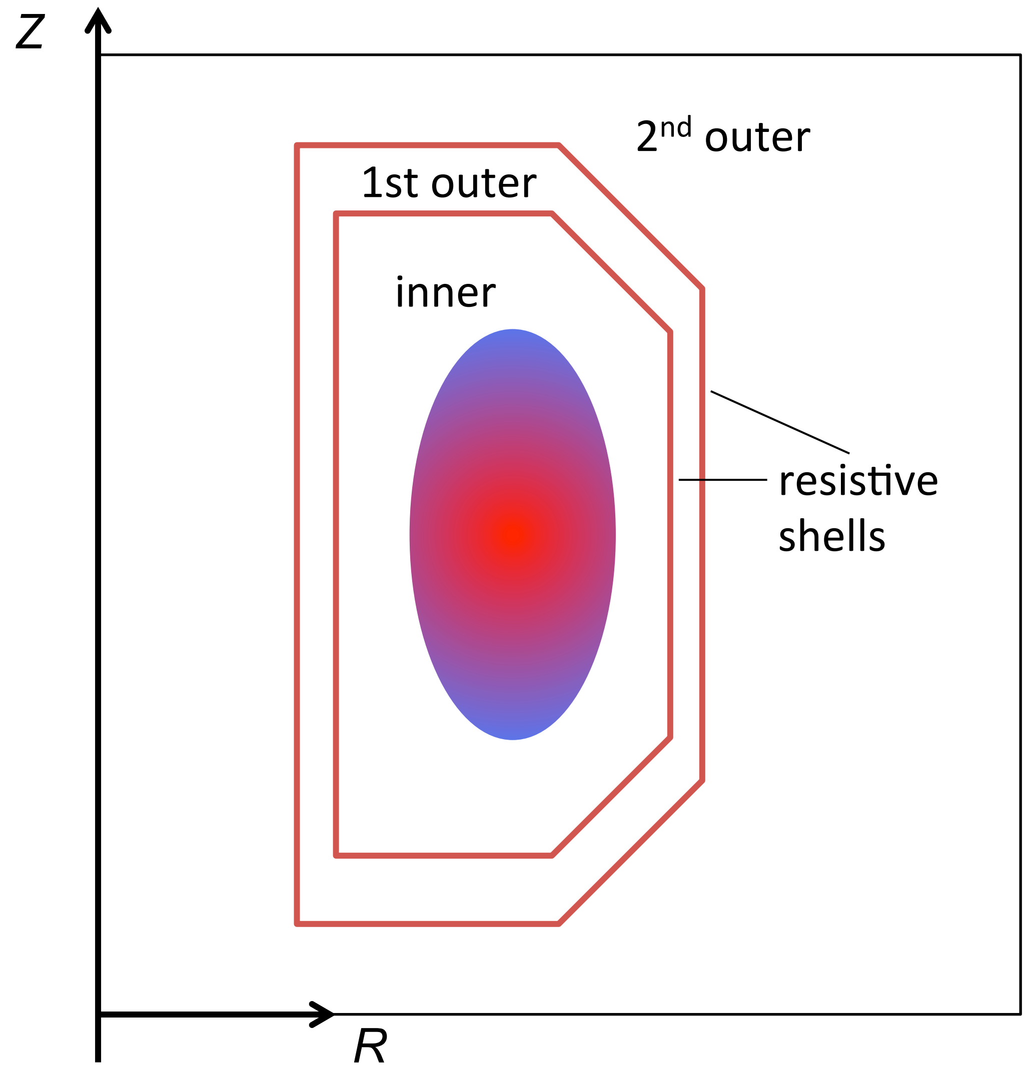

An implicit thin-wall implementation couples the magnetic evolution of different regions.

- In NIMROD's weak form, the PDE from Faraday's law for the interior of each region is

$$\int_R \mathbf{A}^* \cdot \frac{\partial \mathbf{B}}{\partial t} dVol = -\int_R \mathbf{E} \cdot \nabla \times \mathbf{A}^* dVol + \oint_{\partial R} \mathbf{A}^* \times \underline{\mathbf{E}} \cdot \hat{\mathbf{n}} \, dS$$

for all vector test functions

$$\mathbf{A}_{k,n,\nu}(R,Z,\phi) = \alpha_k\left[\xi(R,Z),\eta(R,Z)\right] e^{in\phi}\hat{\mathbf{e}}_\nu(\phi)$$

used in the expansion for magnetic field. Here, $\alpha_k(\xi,\eta)$ is a 2D nodal spectral element, $\hat{\mathbf{e}}_1 = \hat{\mathbf{R}}(\phi), \hat{\mathbf{e}}_2 = \mathbf{Z}, \hat{\mathbf{e}}_3 = \hat{\boldsymbol{\phi}}(\phi)$, and

$$\mathbf{B}(R,Z,\phi,t) = \sum_{k,n,\nu} B_{k,n,\nu}(t)\mathbf{A}_{k,n,\nu}(R,Z,\phi)$$

The resistive-wall $\underline{\mathbf{E} = v_w \hat{\mathbf{n}} \times \delta \mathbf{B}}$ is used in the surface integral. $v_w \equiv \dfrac{\eta_w}{\mu_0 \delta x}$

Evolution of the normal component is imposed as an integral constraint with the same test functions.

- Applying Faraday's law along an interface between regions,

$$\int_{\partial R} \mathbf{A}^* \cdot \hat{\mathbf{n}}\hat{\mathbf{n}} \cdot \frac{\partial \mathbf{B}}{\partial t} dS = -\int_{\partial R} \mathbf{A}^* \cdot \hat{\mathbf{n}}\hat{\mathbf{n}} \cdot \nabla \times \mathbf{E}\, dS$$

$$= \int_{\partial R} \hat{\mathbf{n}} \cdot \nabla\left(\mathbf{A}^* \cdot \hat{\mathbf{n}}\right) \times \mathbf{E}\, dS - \sum_j \oint_{\partial R_j} \mathbf{A}^* \cdot \hat{\mathbf{n}}\, \mathbf{E} \cdot d\mathbf{l}$$

with path integrals defined by curves swept by the corners of the 2D elements.

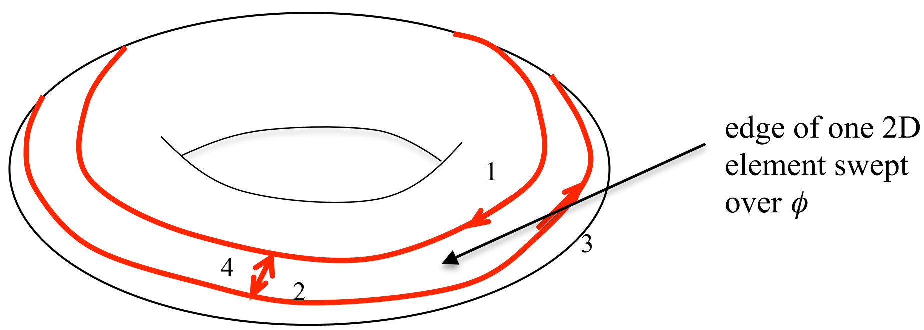

- Adding the constraint equation with a Lagrange multiplier λ provides an un-split relation, and **E** has implicit $v_w \hat{\mathbf{n}} \times \Delta\delta\mathbf{B}$ terms. $\left[\Delta f \equiv f(t+\Delta t) - f(t)\right]$

$$\int_R \mathbf{A}^* \cdot \Delta\mathbf{B}\, dVol + \Delta t \int_R \mathbf{E} \cdot \nabla \times \mathbf{A}^*\, dVol - \Delta t \oint_{\partial R} \mathbf{A}^* \times \mathbf{E} \cdot \hat{\mathbf{n}}\, dS$$

$$+ \lambda\left[\int_{\partial R} \mathbf{A}^* \cdot \hat{\mathbf{n}}\hat{\mathbf{n}} \cdot \Delta\mathbf{B}\, dS - \Delta t \int_{\partial R} \hat{\mathbf{n}} \cdot \nabla\left(\mathbf{A}^* \cdot \hat{\mathbf{n}}\right) \times \mathbf{E}\, dS + \Delta t \sum_j \oint_{\partial R_j} \mathbf{A}^* \cdot \hat{\mathbf{n}}\, \mathbf{E} \cdot d\mathbf{l}\right] = 0$$

Implicit resistive-wall **E** leads to an algebraic system that couples all regions during each **B**-advance.

- The resistive wall contributions are not symmetric.
- Preconditioned GMRES is used to solve asymmetric algebraic systems.
- The following approach entails minimal modification:
  - For the purpose of the algebraic solve, define separate degrees of freedom for *each* component of **B** along each interface.
    - Physically, the normal component is continuous across a thin wall.
    - Duplication for distinct degrees of freedom does not affect solvability.
  - Apply matrix-based preconditioning region-by-region.
    - Create preconditioners without the contributions to $v_w \hat{\mathbf{n}} \times \Delta\delta\mathbf{B}$ from a neighboring region.
    - Rely on GMRES iteration to provide neighbor contributions.
- Computing the neighbor contributions as matrix-free additions to matrix-vector products simplifies the implementation.
- On a resistive-wall mode test, we find:

$v_w \tau_A / r_{pl}$	0.1	1.0	10.	100.
iterations	3	6	12	20

Tests of vertical stability consider large R/a for comparison with the decay-index criterion.

- The analysis of Mukhovatov and Shafranov [NF **11**, 605 (1971)] treats the tokamak as a loop of current that preserves poloidal flux as it moves and expands or contracts.
- We use coils that are outside the domain to vary the decay index of the vacuum field.
- The vertical dimension of the domain is also varied.
- Equilibria are computed with NIMEQ [Howell, CPC **185**, 1415 (2014)].
- Unstable, up-down symmetric equilibria are computed over half of the domain with a symmetry condition at Z = 0.

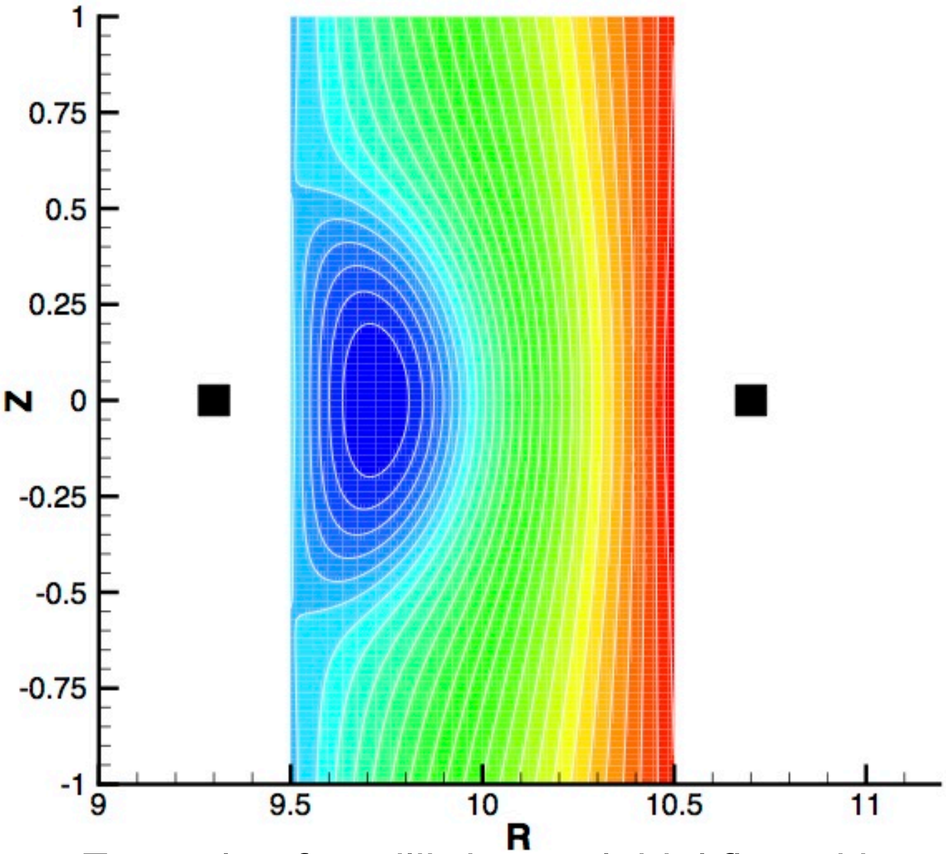

Example of equilibrium poloidal flux with locations of external coils indicated.

Computed linear results show a clear stability threshold when the decay index is varied.

- The decay index N is computed from the vacuum field.

  $$N \equiv -d\ln\left|B_z\right|/d\ln R$$

- These tests have n_0 varying by 10 and P_0 varying by 200 from outside the tokamak to the magnetic axis.
- Resistivity varies as $\eta \sim T^{-3/2}$.
- The Mukovatov-Shafranov threshold for the wire-loop tokamak is $N = 0$.
- Our results are consistent with the analysis when the vertical extent of the domain is sufficiently large.

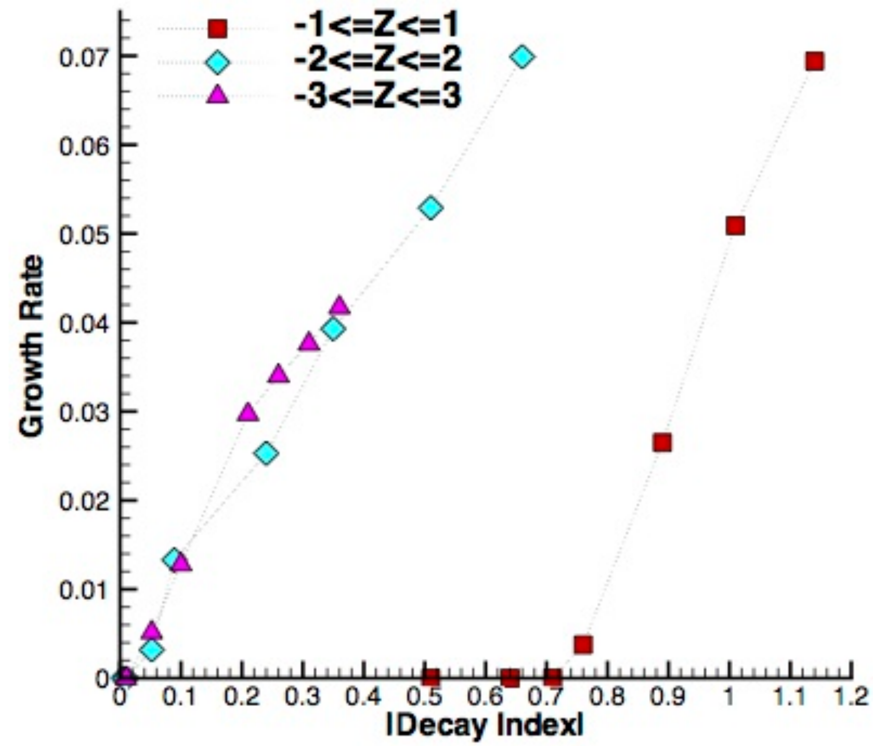

Vertical instability growth rates computed from the linear MHD model with N varied in three sets of computations. [Rates are normalized by $(R_{max}-R_{min})/v_A$.]

Linear VDE computations with different external regions demonstrate resistive-wall scalings.

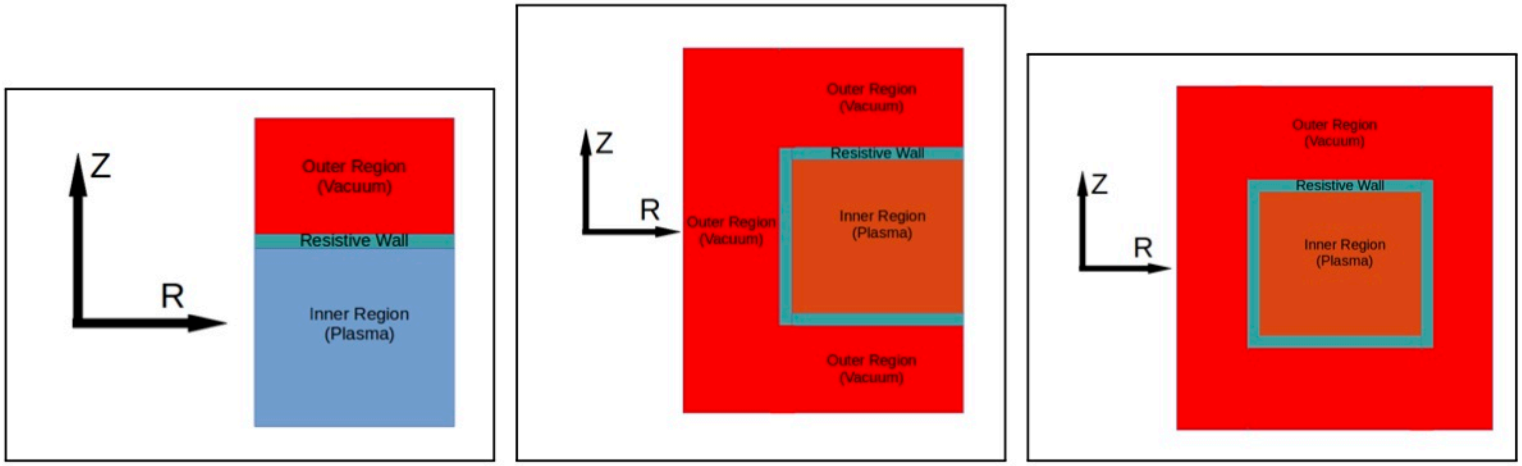

External regions above (left), inboard (center), and surrounding (right) the inner region are illustrated.

Growth rates for N = −0.72 increase with wall resistivity and with the extent of the external region/resistive wall.

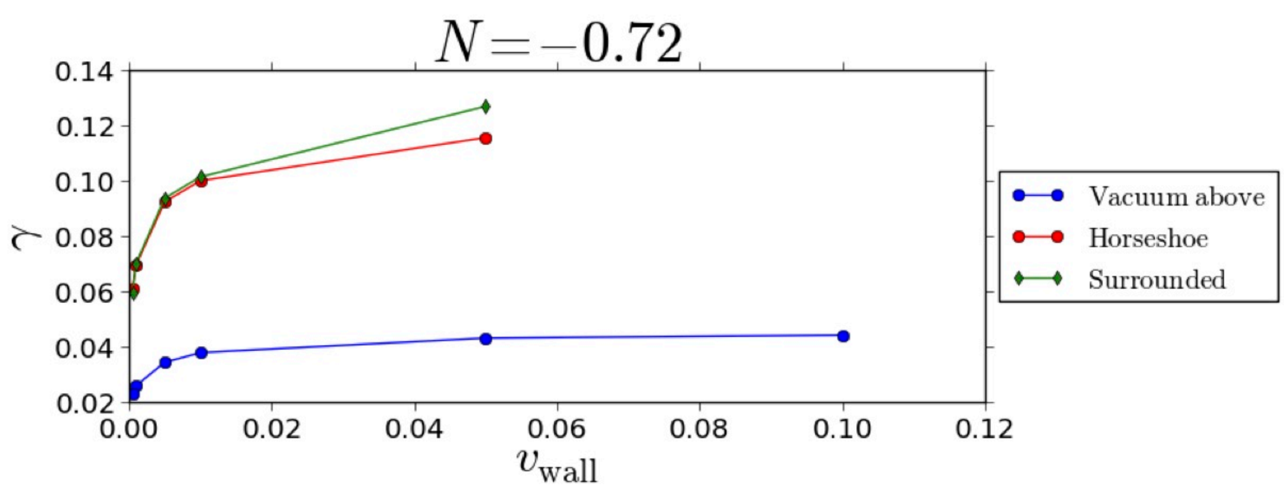

A nonlinear result with conducting walls shows the expected large displacement.

- Parameters are similar to those used for the linear $N = -1.0$ computation, except Pm = 1 instead of 0.1 at the magnetic axis.
- The initial condition is small-amplitude vertical flow.

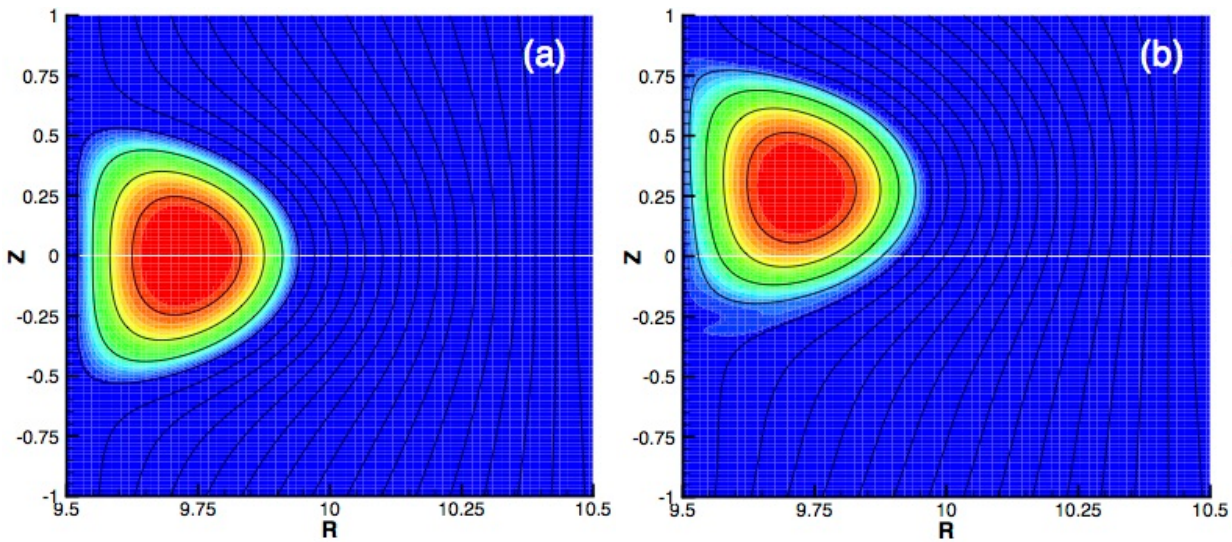

Temperature (color) and poloidal flux (lines) from a nonlinear computation (a) the initial unstable state and at (b) maximum displacement.

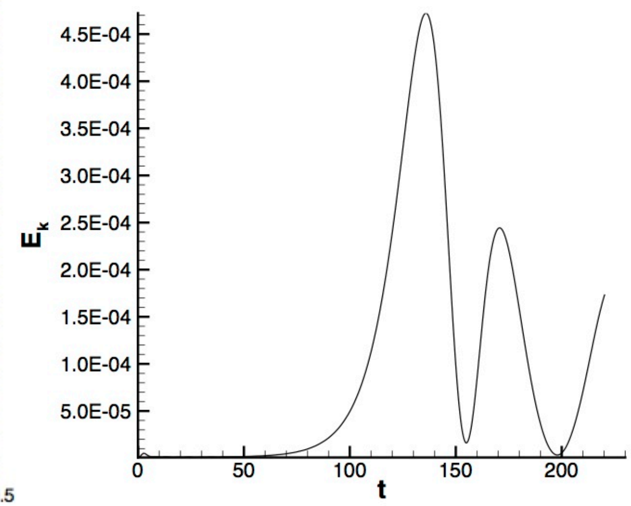

Kinetic energy history shows a linear growth phase and nonlinear evolution with bouncing.

A similar nonlinear computation has an external region above the plasma region.

- The two regions are linked by a thin wall with $v_w = 10^{-3}$.

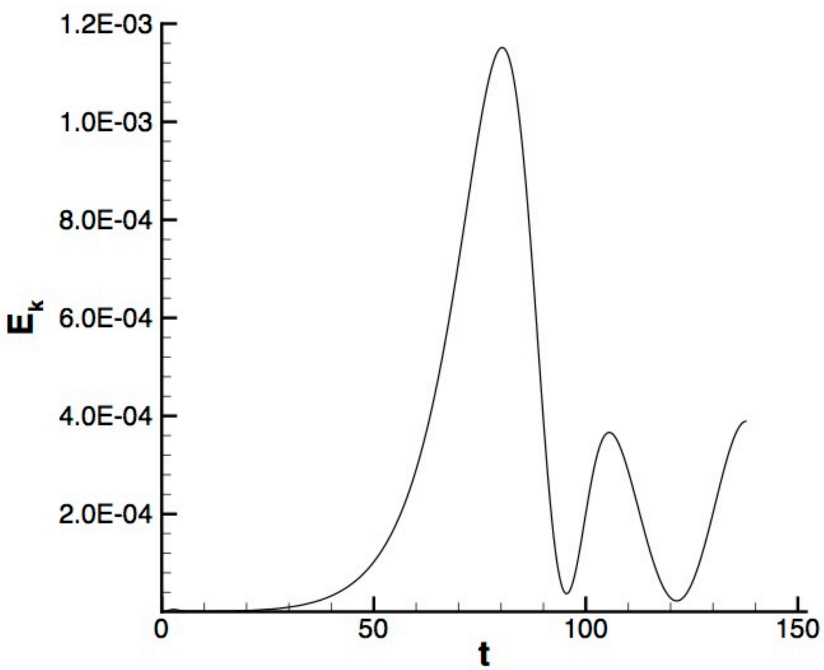

Growth is faster with the resistive wall, and the maximum kinetic energy is larger.

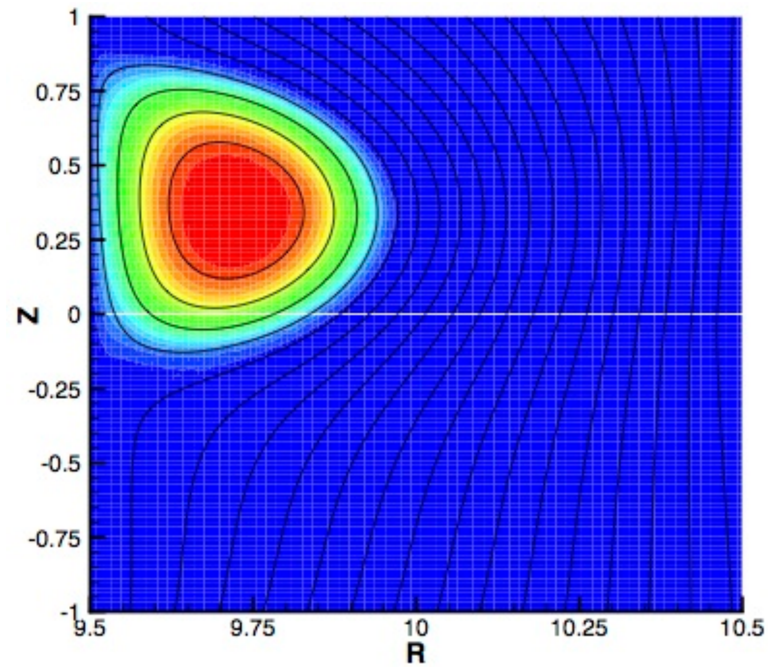

The displaced plasma remains closer to the top surface, and some distortion of poloidal flux, relative to the conducting-wall case, is evident.

We have used an old DIII-D equilibrium to start on modeling realistic cases.

- The computations provide an exercise for importing equilibria as initial conditions.
- The profile is destabilized by imposing external-coil field.

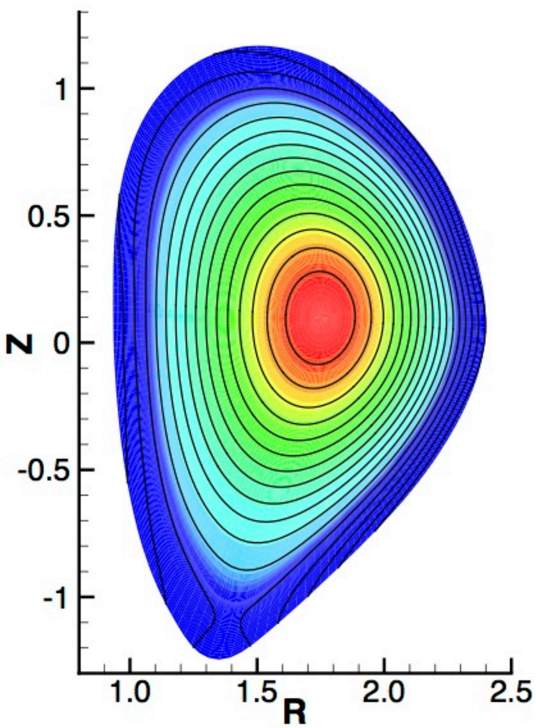

Poloidal flux and pressure contours are aligned in the equilibrium.

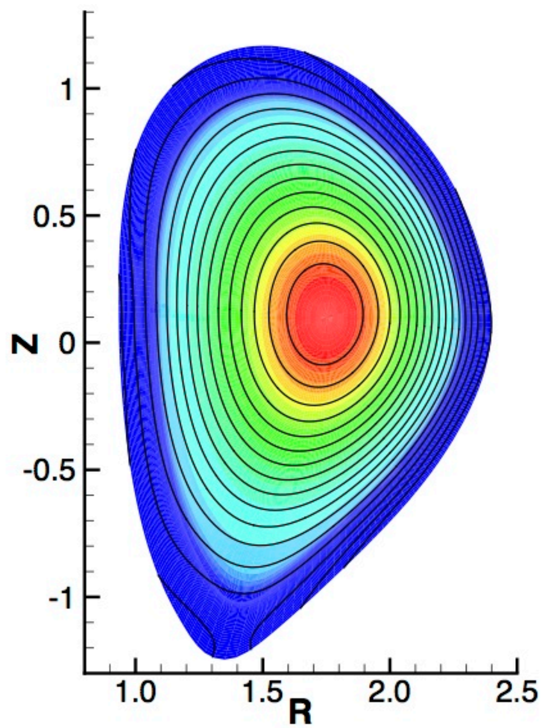

Field from a coil at *R*=1.2, *Z*=-1.5 with I = -0.15 I_p negates some divertor field.

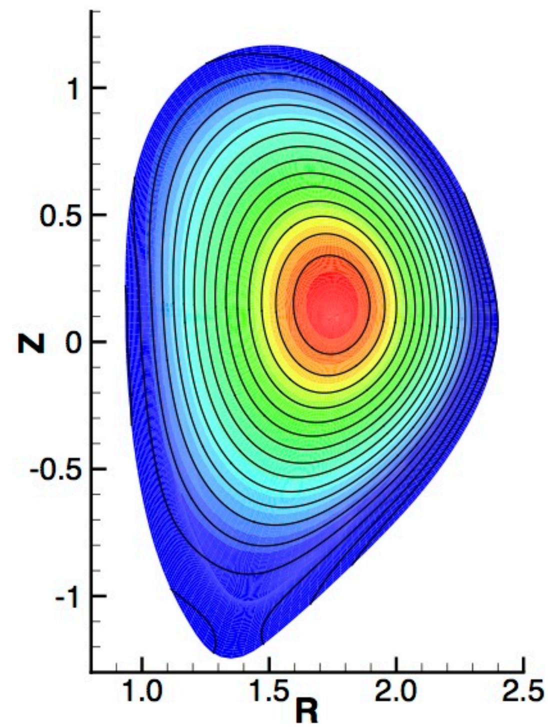

The tokamak drifts upward slowly (t = 480 τ_A).

Discussion and Conclusions

- An un-split implicit formulation of resistive-wall coupling between plasma and vacuum regions has been implemented in NIMROD.
  - B_{norm} evolution along resistive-wall surfaces is applied as a constraint in the advance of magnetic field at each time-step.
  - Matrix-free computations of coupling across resistive walls facilitates iterative solves.
- Verification of linear vertical stability uses large R/a.
  - Results are consistent with the decay-index criterion for sufficiently distant conducting surfaces.
  - Tests with resistive walls and external regions show the expected increase in growth rate with v_w and with the extent of the resistive wall.
- Our first nonlinear VDE results without and with a resistive surface demonstrate Eulerian free-surface evolution.

Discussion (continued)

- Our next development steps are:
  - Add communication calls to the coding for region interfaces to permit parallel computation.
  - Modify boundary conditions for nonzero normal flow.
- Tracking a distorting plasma surface with an Eulerian representation has its challenges.
  - NIMROD has streamline diffusion and thermal conduction for this purpose, but other methods can be applied if needed.
  - Nonlinear external kink has been demonstrated previously.
- Plasma-material interaction effects will be considered.

- **Also see Bunkers and Sovinec, BP8.00016.**

Computations in the outer vacuum regions approximate magnetostatic responses.

- The standard approach uses a magnetic potential.

  $$\mathbf{B} = \nabla\chi, \quad \nabla^2\chi = 0 \text{ in } R_{out} \,, \quad \hat{\mathbf{n}}\cdot\nabla\chi = B_{n_{out}} \text{ on } \partial R_{out}$$

  where χ may be multi-valued in regions that are not topologically spherical.

- The problem may be cast directly in terms of **B** by minimizing

  $$I = \int_{R_{out}} \left[\left(\nabla\times\mathbf{B}\right)^2 + \left(\nabla\cdot\mathbf{B}\right)^2 \right] dVol$$

  over a space of vector functions that satisfy $\hat{\mathbf{n}}\cdot\mathbf{B} = B_{n_{out}}$ on ∂R_{out} .

- A given static solution can also be found as the long-time response to a diffusion problem.

  $$\frac{\partial}{\partial t}\mathbf{B} = \eta_{out}\nabla^2\mathbf{B}$$ subject to $\hat{\mathbf{n}}\cdot\mathbf{B} = B_{n_{out}}$ on ∂R_{out} .

  - This is convenient in NIMROD, which solves the plasma response in terms of **B**.
  - Induction from changes in I_p appear through surface-$\mathbf{E}_{tang}$.
  - Outer-region computations are fast relative to the plasma update.